ACS APPLIED MATERIALS & INTERFACES

Article

Self-assembly with orthogonal imposed stimuli to impart structure and confer magnetic function to electrodeposited hydrogel

Ying Li, Yi Liu, Tieren Gao, Boce Zhang, Yingying Song, Jessica L. Terrell, Nathan Barber, William E Bentley, Ichiro Takeuchi, Gregory F. Payne, and Qin Wang

ACS Appl. Mater. Interfaces, **Just Accepted Manuscript** • DOI: 10.1021/acsami.5b02339 • Publication Date (Web): 29 Apr 2015

ACS Applied Materials & Interfaces is published by the American Chemical Society.
1155 Sixteenth Street N.W., Washington, DC 20036

Self-assembly with Orthogonal Imposed Stimuli to Impart Structure and Confer Magnetic Function to Electrodeposited Hydrogel

Ying Li[1], *Yi Liu*[2,3], *Tieren Gao*[4], *Boce Zhang*[1,§], *Yingying Song*[1], *Jessica L. Terrell*[2,3], *Nathan Barber*[2,3], *William E. Bentley*[2,3], *Ichiro Takeuchi*[4], *Gregory F. Payne*[2,3], *Qin Wang*[1,*]

[1] 0112 Skinner Building, Department of Nutrition and Food Science, University of Maryland, College Park, Maryland 20742, United States

[2] Fischell Department of Bioengineering, University of Maryland, College Park, Maryland 20742, USA

[3] Institute for Bioscience & Biotechnology Research, University of Maryland, College Park, Maryland 20742, USA

[4] Department of Materials Science and Engineering, University of Maryland, College Park, Maryland 20742, USA

[§] Current address: Environmental Microbial and Food Safety Laboratory, United States Department of Agriculture, Beltsville, MD 20705, USA

[*]Corresponding Author. E-mails: wangqin@umd.edu; Phone: (301) 405-8421; Fax: (301)-314-3313.

ABSTRACT

A magnetic nanocomposite film with capability of reversibly collecting functionalized magnetic particles was fabricated by simultaneously imposing two orthogonal stimuli (electrical and magnetic). We demonstrated that cathodic co-deposition of chitosan and Fe_3O_4 nanoparticles while simultaneously applying a magnetic field during co-deposition can (i) organize structure, (ii) confer magnetic properties, and (iii) yield magnetic films that can perform reversible collection/assembly functions. Magnetic field triggered the self-assembly of Fe_3O_4 nanoparticles into hierarchical "chains" and "fibers" in the chitosan film. For controlled magnetic properties, the Fe_3O_4-chitosan film was electrodeposited in the presence of varied strength of magnetic field and different deposition time. The magnetic properties of the resulting films should enable broad application in complex devices. As a proof of concept, we demonstrate the reversible capture and release of green fluorescent protein (EGFP) conjugated magnetic microparticles by the magnetic chitosan film. Moreover, antibody-functionalized magnetic microparticles were applied to capture cells from a sample, and these cells were collected, analyzed and released by the use of the magnetic chitosan film, paving the way for applications such as reusable biosensor interfaces (e.g., for pathogen detection). To our knowledge, this is the first report to apply magnetic field during the electrodeposition of a hydrogel to generate magnetic soft matters. Importantly, simple, rapid and reagentless fabrication methodologies demonstrated here are valuable features for creating a magnetic device interface.

KEYWORDS electrodeposition; nanocomposite film; self-assembly; magnetic nanoparticles; magnetization; reversibly collection; biosensor interface

1. INTRODUCTION

Stimuli-responsive polymers that self-assemble through strong non-covalent interactions are interesting because their hierarchical structure can be controlled by the sequence of cues used to trigger self-assembly.[1-2] Once the structure is formed, the strength of the interactions precludes the structure from "annealing" to a more thermodynamically stable state. Many polysaccharides display such behavior[3] and several studies have demonstrated that complex structures can be generated by imposing a complex sequence of triggering stimuli.[4-8]

Chitosan is a pH-responsive aminopolysaccharide that can be triggered to self-assemble to form a three-dimensional hydrogel structure. Mechanistically, chitosan's amines are protonated at low pH to yield a water-soluble cationic polysaccharide, while an increase in pH can trigger chitosan's self-assembly by a deprotonation reaction that induces a reversible sol-gel transition. Over a decade ago, chitosan was observed to electrodeposit at a cathode by the neutralization mechanism illustrated in **Scheme 1a**: [9-15] the imposed cathodic input yields a high pH adjacent to the cathode surface and this serves to deprotonate chitosan's amine and induce the localized gelation of chitosan at the cathode surface.[3, 16] More recent studies demonstrate that the structure[8] and properties[17] of the electrodeposited chitosan film can be controlled by the conditions used to trigger self-assembly which is consistent with the electrodeposited hydrogel being stabilized by strong non-covalent interactions. Importantly, several groups have demonstrated that various particles can be co-deposited with chitosan and entrapped within the hydrogel network. For instance, the entrapped particles could be proteins (e.g., enzymes) to confer biological function to the deposited chitosan film (e.g., for biosensing).[11-12, 18] In addition, synthetic particles could be entrapped (e.g., Pt-Pb, Fe_3O_4, MnO_2 and Au nanoparticles) to confer electrical function to the film (e.g., to facilitate signal transduction).[6, 19-22]

Here we report the use of two orthogonal imposed stimuli to self-assemble a composite film with magnetic properties. As illustrated in **Scheme 1b** we first suspend magnetic Fe_3O_4 nanoparticles (MNPs) in a chitosan solution and then impose an electrical input to trigger chitosan's cathodic electrodeposition. During deposition, we simultaneously impose a magnetic signal that serves to organize the Fe_3O_4 nanoparticles. Specifically, we demonstrate that electrodeposition in the presence of an imposed magnetic field: (i) organizes the hierarchical structure of the nanoparticles within the electrodeposited chitosan hydrogel film, (ii) confers magnetic properties to the film, and (iii) yields magnetic films that can reversibly capture biologically-based magnetic particles.

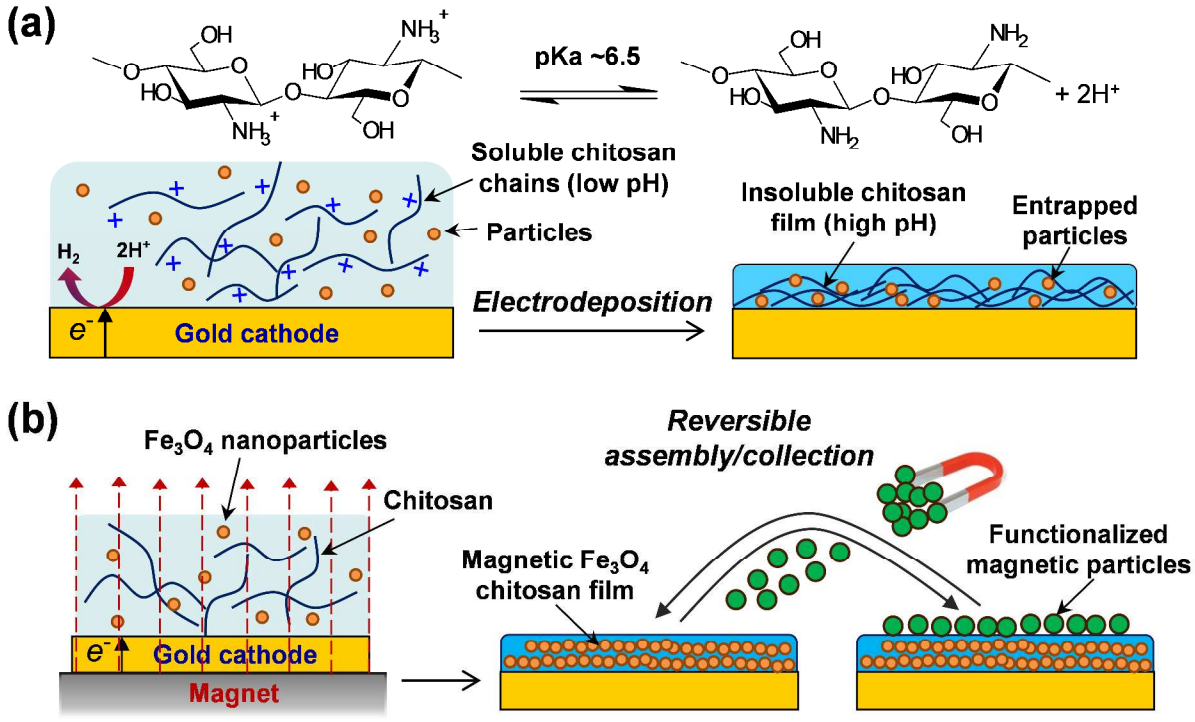

Scheme 1. (a) Mechanism of co-electrodeposition of pH-responsive chitosan and magnetic nanoparticles at a cathode. The entrapped particles are randomly distributed within the film

when co-deposition was performed in the absence of an applied magnetic field. (b) Simultaneous imposition of a magnetic field during co-deposition can (i) organize structure, (ii) confer magnetic properties, and (iii) yield magnetic films that can perform reversible assembly/collection functions.

2. EXPERIMENTAL SECTION

2.1 Preparation of cast MNP-chitosan film

Chitosan solution (1 % w/w, pH 5.3) was prepared as previously reported.[3] The synthesis of amine-functionalized MNPs was reported by Wang, et al.[23] The detailed synthetic procedures and characterization of the MNPs can be seen in supporting information.

The MNP-chitosan suspension was prepared by sonicating and vortexing 10 mg MNPs in 10 ml chitosan solution for 30 min, and then casting on a piece of aluminum sheet, under which a magnet disc was placed. The casted MNP-chitosan film was then dried under ambient conditions all under influence of with imposing magnetic field from the magnet disc. Three types of N48 neodymium magnets (Apex Magnets, Petersburg, WV) were used, namely, 1.27 *d* ×0.318 *h* cm disc, 1.27 *d* ×0.635 *h* cm disc, and 1.27 *d* ×1.27 *h* cm cylinder. The distance between the magnets and the aluminum sheet was adjusted using non-magnetic material to obtain the target magnetic field strength that was measured by a hand-held gaussmeter (Model 410, Lake Shore Cryotronics, Inc.). Cast MNP-chitosan films without applying an external magnetic field were prepared as control.

2.2 Electrodeposition of chitosan and MNP-chitosan films

A piece of 5 mm thick polydimethylsiloxane (PDMS) with a punched hole (8 mm in diameter) was placed on top of a gold coated quartz electrode (International Crystal Manufacturing) and assembled with or without a magnet under the electrode. Two hundred microliter chitosan solution (1.0 %, pH 5.3) or MNP-chitosan suspension (0.8 mg MNPs/ml) was pipetted on top of the gold electrode and a Pt wire counter electrode was immersed into the deposition solution. Electrodeposition was initiated by biasing the gold electrode as a cathode using a DC power source (2400 Sourcemeter, Keithley Instruments, Inc.,). Detailed information about deposition time and applied magnetic field was provided in the text.

2.3 Characterization of MNP-chitosan films

The experimental procedures for X-ray diffraction crystallography analysis are provided in supporting information.

Scanning electron microscopy (SEM) images were obtained from a Hitachi SU-70 SEM microscope. Film samples were adhered to a 1-inch specimen stub with conductive carbon tape (Electron Microscopy Sciences). A thin layer of gold and platinum was then coated on the samples using a sputter coater (Hummer XP). Energy dispersive X-ray (SEM-EDS) mapping was obtained using a Bruker SOL-XE detector (Bruker AXS Inc.). In SEM-EDS spot analysis, representative points in the elemental map were randomly selected to investigate the elemental composition. The distribution of four elements (C, N, O and Fe) and their relative content in samples were reported.

Magnetic properties of MNPs, MMPs and MNPs-chitosan films were measured by a vibrating sample magnetometer (VSM, 7400, Lake Shore Cryotronics, Inc.). The powdered MNPs and MMPs were filled inside a Kel-F sample holder cup (Lake Shore Cryotronics, Inc.).

The film-coated gold electrodes or aluminum sheets were attached to a Kel-F thin-film bottom sample tail (Lake Shore Cryotronics, Inc.) by cellophane tape. All experiments were conducted at 25°C.

2.4 Conjugation of protein and antibody to MMPs

Preparation and purification of enhanced green fluorescent protein (EGFP) has been reported previously.[24] Briefly, recombinant *Escherichia coli* (*E. coli*, BL21(DE3)) bearing pET-eGFP-7K (kanamycin-resistant plasmid) was used for the production of EGFP (His-tagged). Extraction of EGFP and purification using His affinity agarose Co-NTA Agarose (Cube Biotech) were performed following the product protocols. For conjugation of antibody to MMPs, Polyclonal *E. coli* serotypes O + K antibody (Goat / IgG, PA1-27226, Pierce Biotechnology, Inc.) was used.

EGFP or antibody was conjugated on MMPs through carboxyl activating agent 1-ethyl-3-(3-dimethylaminopropyl) carbodiimide (EDC). The reaction was carried out in 2-(N-morpholino)-ethanesulfonic acid (MES) buffer. Firstly, 1 mg MMPs, 300 µl MES (pH 5.2) and 35 µl of EDC solution (2 mg/ml in pH 5.2 MES buffer) were mixed for 30 min, and then the activated MMPs were separated from the liquid by applying a magnet to the container. Secondly, the activated MMPs was mixed with 150 µl EGFP solution (1 mg/ml in pH 7.2 MES buffer) or 100 µl *E.coli* antibody solution (1 mg/ml in pH 7.2 PBS buffer) in dark at 25°C for 4 h. Finally, the resulting MMP-EGFP or MMP-antibody conjugates was magnetically separated and re-suspended in 1 ml MES buffer (pH 7).

2.5 Statistical analysis

All measurements were carried out in triplicates. The results were expressed as means. For statistical analysis, the data were subjected to analysis of variance ($P < 0.05$) followed by Tukey's test with an experiment-wise confidence level of $\alpha=0.10$, using SAS 9 software (SAS Institute Inc.).

3. RESULTS AND DISSCUSION

3.1 Casting MNP-chitosan film: the alignment of magnetic nanoparticles

3.1.1 Structural evidence of magnetic alignment of MNPs in the cast film

In our initial tests, we examined the effect of external magnetic field on the MNPs in cast chitosan film. **Figure 1a** schematically illustrates the MNP-chitosan film casting procedures in the presence/absence of applied magnetic field. MNP-chitosan film in the presence of a magnetic field was prepared by dropping 20 μl of well-suspended MNPs (1 mg/ml) in chitosan solution (1 %, pH 5.3) on an aluminum sheet that has a magnet disc underneath. The cast MNP-chitosan film was allowed to dry at room temperature overnight and the magnetic field was applied during the whole process. Control film was prepared in the same way except no magnetic field was applied.

Figure 1b shows the structure of the cast MNP-chitosan film without magnetic alignment. The left two images are photographs of the cast film showing uniformly distributed MNPs in chitosan. The SEM images on the right of **Figure 1b** show that the discrete MNPs were randomly embedded in the film. On the other hand, MNP-chitosan films casted in the presence

of a magnetic field showed highly ordered patterns. The photographs on the right of **Figure 1c** show uneven distribution of MNPs in the film. The SEM images in **Figure 1c** show groups of fiber-like structures and almost all the MNPs in the films were completely aligned into chains without disorderly located ones. The magnified SEM image (right most in **Figure 1c**) shows that the fibers were composed of straight necklace-like chains, which consisted of spherical MNPs. The texture of chitosan layer can also be seen on top of the MNP chains, suggesting that the MNP chains were pulled away from the surface and embedded deeper into the chitosan film.

3.1.2 Chemical evidence of magnetic alignment of MNPs in the cast film

The effect of the external magnetic field on MNPs alignment in chitosan film can also be examined using SEM-EDS elemental mapping analysis. **Figure 1d** shows that the MNP-chitosan film without magnetic alignment has homogeneous distributions of iron and carbon. This suggests that the MNPs were well dispersed in the film and that the magnetic moments of the MNPs in the film were randomly oriented.

Figure 1e shows that the MNP-chitosan film with magnetic alignment has enriched areas of iron and carbon. The distribution of iron corresponds to the presence of MNPs chains seen in the SEM image on the left. The wide spread signal of carbon suggest the layout of chitosan covered the most area in the film. Taken together, **Figure 1** demonstrates that external magnetic field can trigger the self-assembly of MNPs into long-range ordered chains, and further created hierarchical parallel clusters of the assembled chains over large areas in the chitosan film. The linking of the MNPs was possibly driven by magnetostatic interactions.[25]

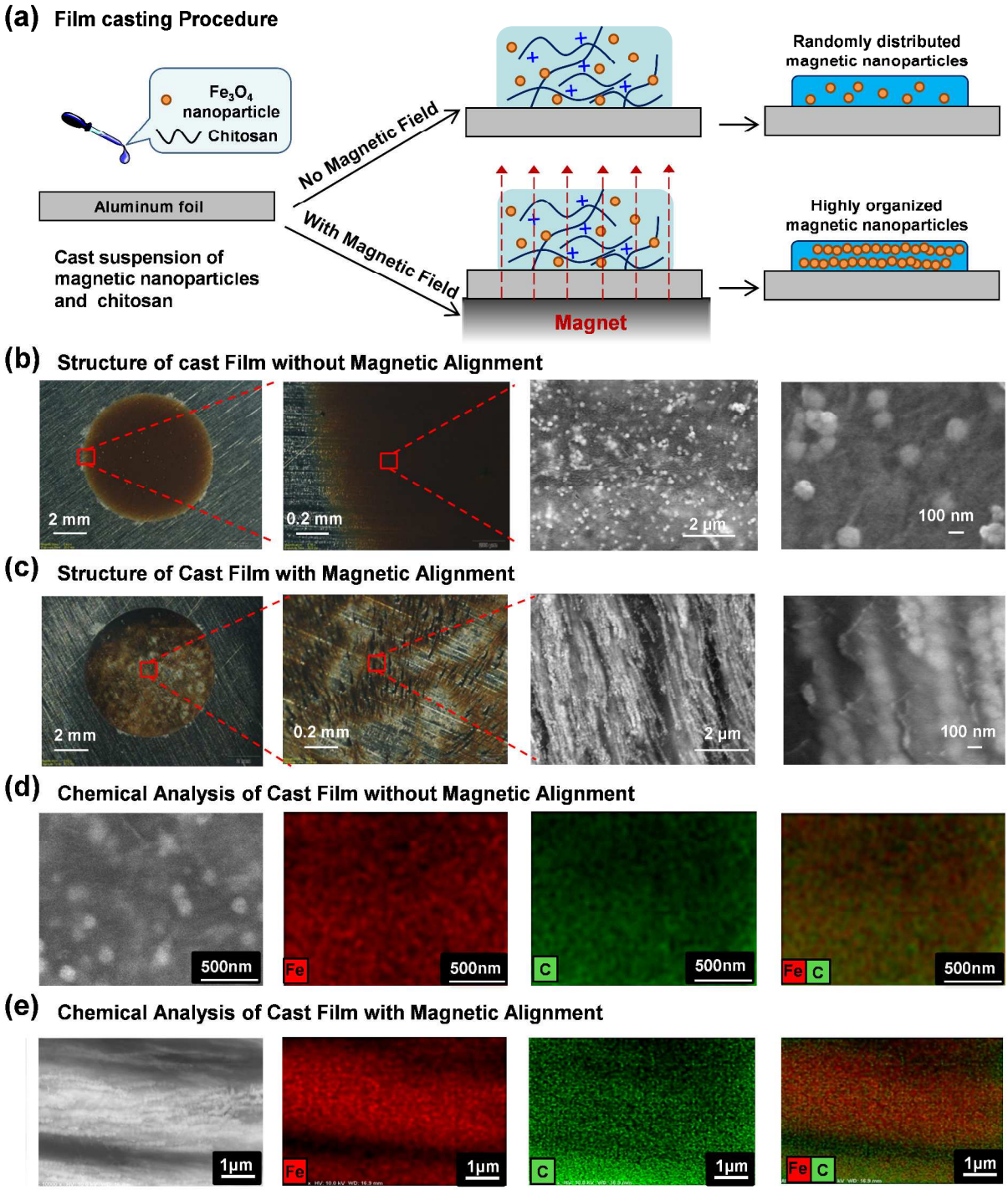

Figure 1. (a) Schematic illustration of film casting procedures in the presence/absence of applied magnetic field. (b) Structure of cast films without magnetic alignment. (c) Structure of cast films with magnetic alignment. (d) Chemical analysis of cast films without magnetic alignment. (e)

Chemical analysis of cast films with magnetic alignment. The images were taken in top-down view by optical microscopy and SEM.

3.2 Electrodeposition of MNP-chitosan film: the simultaneous application of electrical stimuli and magnetic field

3.2.1 Electrodeposition of MNP-chitosan film

Electrodeposition of chitosan films showed unique advantages in creating micro-devices in that this directed assembly process can be controlled spatially and temporally.[26] To co-electrodeposit MNPs and chitosan, the gold-coated quartz electrode was assembled as schematically illustrated in **Figure 2a** and exposed to MNPs-chitosan suspension. For magnetic alignment experiments, a magnet was placed under the electrode to create a magnetic field. Because the electrode was centered and much smaller than the magnet, the direction of the applied magnetic field could be considered out of plane. Electrodeposition was initiated by applying a constant current density of 3 A/m^2 to the gold cathode for 4 min in the presence of the magnetic field. After electrodeposition, the film was gently rinsed with water to remove un-deposited materials and air-dried overnight in ambient conditions. The magnet was removed after the films were dried. The control films were prepared without using magnets during the entire process.

3.2.2 Structural evidence of magnetic alignment and increased accumulation of MNPs in MNP-chitosan film during electrodeposition

Electrodeposited MNP-chitosan films without magnet alignment were observed to be translucent with scattered black particles (left photograph in **Figure 2b**). SEM images in **Figure**

2b show a homogeneous distribution of spherical MNPs in the film, indicating these particles were well dispersed without aggregation. This is consistent with the cast MNP-chitosan film prepared without applying an external magnetic field. Presumably, the magnetic moments of MNPs are randomly oriented in the film.

On the other hand, electrodeposited MNP-chitosan films with magnetic alignment display dramatic structural difference compared to those deposited without alignment. Films with magnetic alignment (left photograph in **Figure 2c**) were much darker than those without magnetic alignment (**Figure 2b**), indicating more MNPs were deposited in the presence of the external magnetic field, presumably due to magnetic attraction between MNPs and the magnet under the electrode. SEM images in **Figure 2c** show crowded "fibers" which consisted of MNP chains throughout the film. Magnified SEM images in **Figure 2c** clearly show that MNPs form highly ordered parallel chains and the particles themselves orient along the chain.

3.2.3 Chemical evidence of magnetic alignment and concentrating of MNPs in MNP-chitosan film during electrodeposition

SEM-EDS analysis provided chemical evidence for the co-electrodeposition of MNPs and chitosan, and the significant aligning effect of the magnetic field during electrodeposition. **Figure 2d** shows that without magnetic alignment during the electrodeposition, the iron signals are randomly distributed throughout the films, indicating good dispersion of MNPs in the film. Carbon signals are also uniformly distributed, corresponding to the observation that MNPs are randomly embedded in the chitosan film for the non-aligned cases. On the other hand, **Figure 2e** shows that strong iron signals coincide with the MNPs fibers as shown in the SEM image on the

left for the electrodeposited MNP-chitosan film with magnetic alignment. In addition, carbon signals dominate areas other than the dense MNP fibers, indicating that these fibers were on the surface of the film or replaced chitosan.

To evaluate the variations of MNPs amounts in the MNP-chitosan films, SEM-EDS elemental quantitative analysis was conducted by randomly probing various spots in the examined SEM area and the results are shown in **Table 1**. The amount of MNPs in the suspension for casting film were the same in the presence or absence of magnetic field, thus it is not surprising that the relative atomic ratios of iron in both films were reasonably close to each other. On the other hand, the iron ratio in the electrodeposited film with magnetic alignment was remarkably higher than that in the film without magnetic alignment, providing chemical evidence for the enrichment effect of the magnetic field on the assembly of MNPs in the chitosan film during the electrodeposition process.

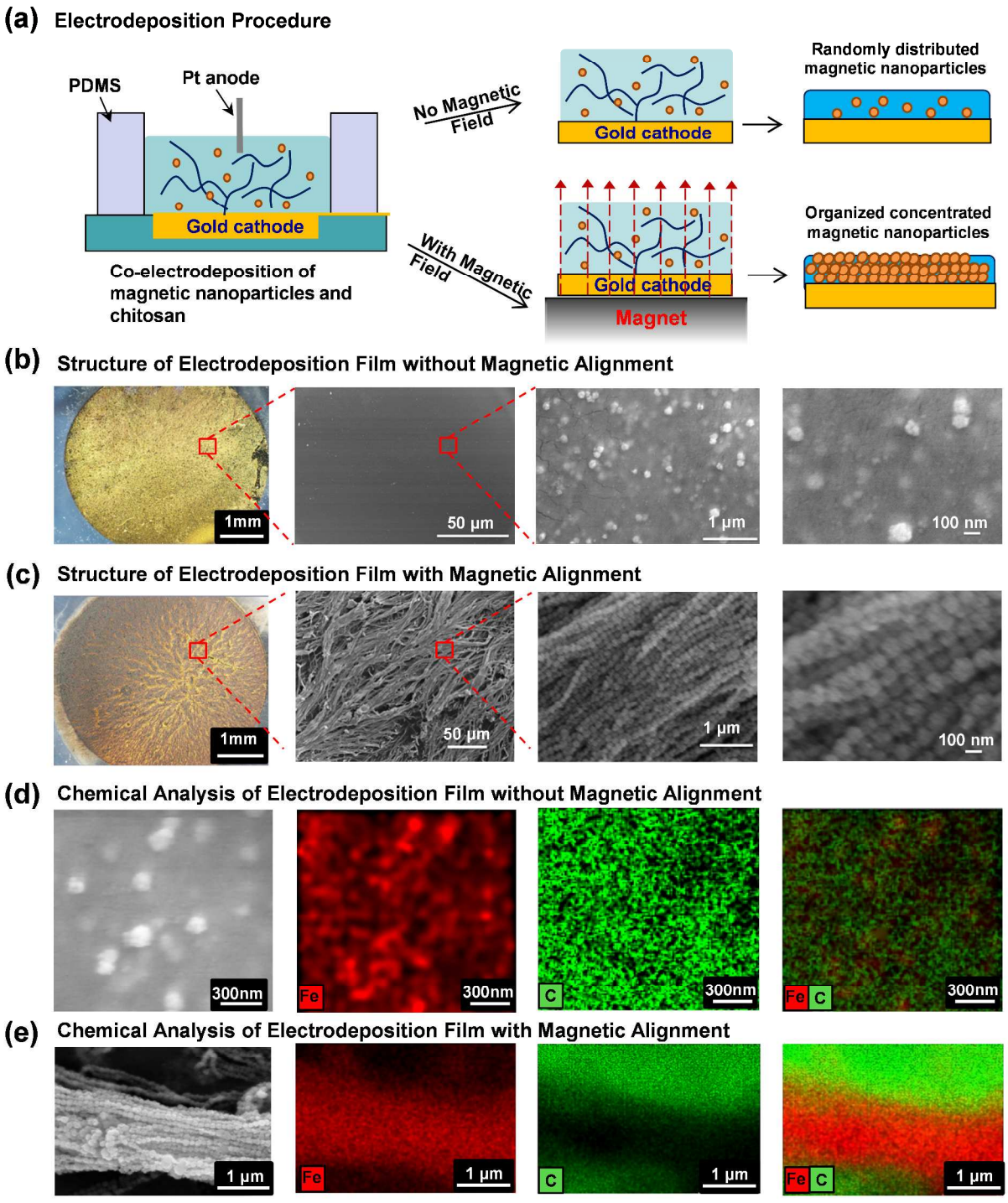

Figure 2. (a) Schematic illustration of film electrodeposition procedures in the presence/absence of a magnetic field. (b) Structure of electrodeposited films without magnetic alignment. (c) Structure of electrodeposited films with magnetic alignment. (d) Chemical

analysis of electrodeposited films without magnetic alignment. (e) Chemical analysis of electrodeposited films with magnetic alignment. The images were taken in top-down view by optical microscopy and SEM.

Table 1. SEM-EDS analyses of normalized average atomic ratio (%) of C, N, O and Fe in the MNP-chitosan films fabricated by electrodeposition or casting in the presence or absence of magnetic field (MF) *

Element	Electrodeposited film without MF	Electrodeposited film with MF	Casting film without MF	Casting film with MF
C	31.4±8.5	22.1±0.9	35.0 ± 2.6	31.2±1.7
N	28.6±9.2	17.3±0.8	23.9±2.2	18.4±1.3
O	39.6±14	30.9±1.57	29.6±2.6	35.1±2.3
Fe	0.25±0.10	29.7±0.2	11.5±0.1	15.3±0.4

*Data were expressed as mean percentage ± standard error of the mean.

3.3 Control of magnetic properties of the film during the deposition process

3.3.1 Magnetic properties of cast MNP-chitosan films

Magnetic properties of magnetic materials are often evaluated by hysteresis loops,[27] which can be obtained from a vibrating sample magnetometer. From the hysteresis loops one can obtain: 1) saturation magnetization (M_s), which represents a state where an increase in applied external magnetic field cannot further increase the magnetization of the material; 2) remanent magnetization (M_r), which indicates how much magnetization has been retained when the externally applied field is brought to zero after magnetic saturation has been attained; and 3) coercivity H_c. In addition, the value of M_r/M_s, the squareness ratio, measures how square a

hysteresis loop is and it reflects the easy/hard trend of magnetization reversal. Hysteresis measurements of our MNP-chitosan films were recorded with a static magnetic field applied either parallel (in-plane) or normal (out-of-plane) to the plane of the film. The value of M_s was considered as in-plane magnetization measured at magnetic field of 3 kOe. As shown in **Figure S2a**, the representative in-plane and out-of-plane hysteresis loops of the film casted with a 3.5 kOe indicate that the easy axis of the film lie in the film plane, which is consistent with other thin films containing iron or magnetite.[25, 28]

First, in order to investigate the effects of magnetic alignment on the magnetic properties of cast MNP-chitosan films, we compared in-plane hysteresis loops of cast MNPs-chitosan films with or without magnetic alignment. As shown in **Figure 3a**, M_s of the film with magnetic alignment (3.5 kOe field) is slightly higher (~ 6%) than the film without magnetic alignment. Importantly, M_r of cast MNP-chitosan film with magnetic alignment is much higher (2-fold) than that without magnetic alignment, indicating that the magnetic moments of MNPs in the cast film are partly aligned in the film plane.

Next we investigate whether the magnetic properties of the MNP-chitosan film are tunable by varying the strength of the applied magnetic field. The M_s of all the aligned films were not significantly different (data not shown). **Figure 3b** shows M_r and M_r/M_s measured in the film plane, whereas **Figure 3c** shows those measured out of the film plane. It can be seen that the M_r and M_r/M_s measured in-plane increase as a function of applied magnetic field during casting and are remarkably larger than those measure out-of-plane, although the magnetic field was applied out of the film plane. We offer the following explanation about the results in **Figure 3b** and **3c**.

Commonly, the magnetic moments of magnetic materials tend to align along the applied field.[29-32] For an individual particle, magnetic energy is the lowest when magnetic moment is

oriented along the applied field directions.[33] However, because the easy axis of the MNPs chains lay in in-plane, to alter the direction of their magnetic moments to out-of-plane direction, the strength of an applied magnetic field has to overcome the sum of demagnetization field, chain-chain interactions field and magnetocrystalline anisotropy field. The demagnetization field is expressed as[34]

$$H_d = - N_d M$$

where N_d is the global demagnetizing factor, and M is the magnetization of the MNPs. N_d=1 along the chain direction for chains embedded in a thin film.[34] The demagnetization field was evaluated to be 4.5 kOe using magnetization of 354 emu/cm³ with the density of Fe_3O_4 5 g/cm³. Secondly, the magnetostatic interactions among particles and chains greatly increase the difficulty of domain rotation.[25] Therefore, the force needed to orient the magnetic moments to out-of-plane direction was speculated to be far greater than 4.5 kOe, which was the largest field strength applied in this study. Thirdly, magnetocrystalline anisotropy might be contributing to the easy axis alignment although it is small.[35] In summary, an applied field must exceed a certain critical value for irreversible rotation of magnetic moment to occur.[36] Therefore, it was favorable for the MNP chains to align in the film plane despite the direction of the applied field was perpendicular to the film plane.

For films casted in 1 kOe field, the M_r and M_r/M_s measured in both directions were significantly higher than the non-aligned film (**Figure 3b** and **3c**), probably because the MNPs were magnetized and self-assembled into ordered structures for aligned films. Interestingly, in the range of 1-4.5 kOe, the M_r and M_r/M_s in the plane of the films increased as a function of magnetic field strength, while those parameters of the film measured in the out-of-plane direction decreased. The value of out-of-plane M_r and M_r/M_s of the films casted in a 4.5 kOe field

decreased to almost the same as those of non-aligned films. This trend suggested that the cast MNP-chitosan film was more easily magnetized along the film plane with increasing field. In addition, increasing the field strength may have an impact on aligning the easy axis of the MNPs chains to a certain direction within the plane.

(a)

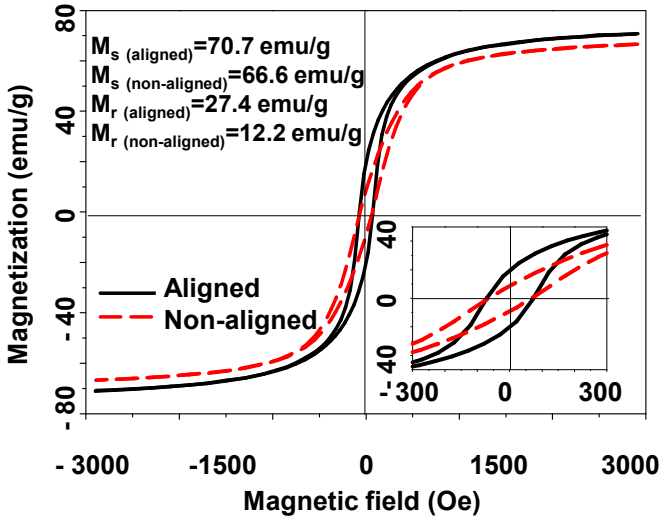
$M_{s\ (aligned)}$=70.7 emu/g
$M_{s\ (non-aligned)}$=66.6 emu/g
$M_{r\ (aligned)}$=27.4 emu/g
$M_{r\ (non-aligned)}$=12.2 emu/g
Aligned
Non-aligned
Magnetization (emu/g)
Magnetic field (Oe)

(b)

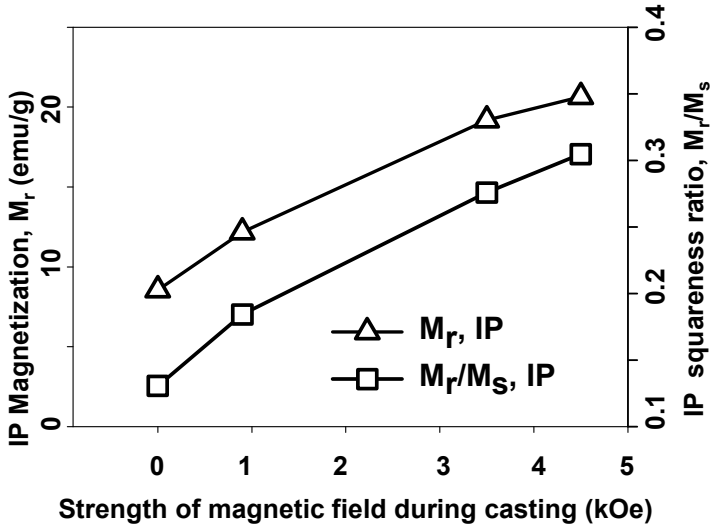
M_r, IP
M_r/M_S, IP
IP Magnetization, M_r (emu/g)
IP squareness ratio, M_r/M_s
Strength of magnetic field during casting (kOe)

(c)

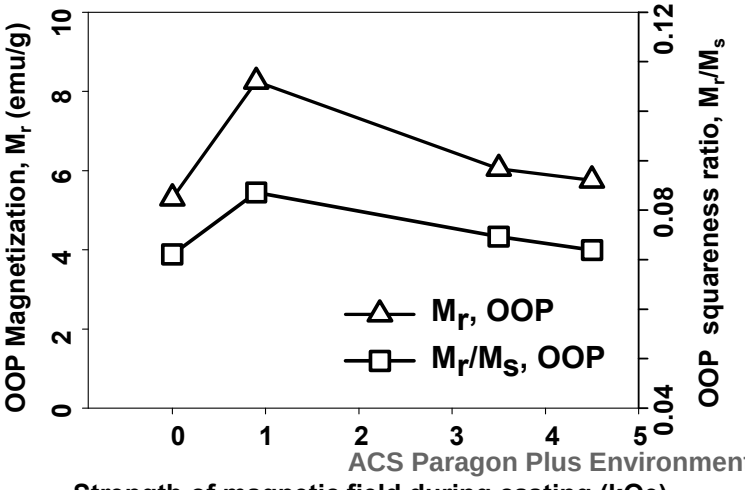
M_r, OOP
M_r/M_S, OOP
OOP Magnetization, M_r (emu/g)
OOP squareness ratio, M_r/M_s
Strength of magnetic field during casting (kOe)

Figure 3. (a) Representative hysteresis loops of cast MNPs-chitosan films with (solid line) or without (dash line) magnetic alignment (3.5 kOe field) measured parallel to the film plane. The inset represents a detail of the hysteresis loops in the low field region. (b) The in-plane remanence (M_r) and squareness ratio (M_r/M_s) of casted films as a function of strength of external magnetic field. (c) The out-plane remanence and squareness ratio of casted films as a function of strength of external magnetic field. The amount of MNPs was 20 μg in all the films. IP, in-plane; OOP, out-of-plane.

3.3.2 Magnetic properties of electrodeposited MNP-chitosan films

3.3.2.1 The effect of external magnetic field on the magnetic properties of electrodeposited films

Electrodeposited MNP-chitosan films were prepared by adding the MNP-chitosan suspension (0.8 mg /ml in 1.0% chitosan) on top of the gold electrode and electrodeposition was initiated by biasing the gold electrode as cathode (3 A/m^2) for 4 min. During the deposition and subsequent washing and drying, magnet discs with varying magnetic field strength were placed under the gold electrode to tune the magnetic field. Unlike the cast MNP-chitosan films, the amount of MNPs in deposited films depends on the deposition conditions. Therefore, the total magnetic moments (m_r and m_s) were used to evaluate the effects of strength of external magnetic field on the magnetic properties of the films. The value of m_s was considered as in-plane magnetic moment measured at 3 kOe. As shown in **Figure 4a**, m_s of the films increased as a function of the strength of external magnetic field, indicating that more MNPs were deposited on the electrode surface with increasing the magnetic field strength of magnet disc.[37]

Figure 4b shows that the in-plane m_r of the films increased almost linearly with the strength of applied magnetic field, whereas out-of-plane m_r remain nearly constant. Also, the in-plane m_r

of the films deposited in the presence of 1 to 4 kOe magnetic field was significantly higher than that of the corresponding out-of-plane m_r, probably due to the predominant alignment of the MNPs chains in the film plane. This is consistent with our observation for the casted MNP-chitosan films (**Figure 3b** and **3c**). The increased in-plane m_r might arise from the combination effects of (1) increased amount of MNPs electrodeposited on the electrode surface; and (2) more magnetic moments of the MNPs were aligned toward a certain direction in the plane. Because the easy axis of the electrodeposited film was in-plane (**Figure S2b**), the limited increase of out-of-plane m_r was probably due to the difficulty in reversal of the magnetic moments from in-plane to out-of-plane, as demonstrated for the casted films (**Section 3.3.1**).

It is shown in **Figure 4c** that the applied magnetic field differentially impacted the in-plane and out-of-plane m_r/m_s of the electrodeposited films. Because m_r/m_s is a normalized value, we showed that the trend of m_r/m_s was indeed independent of the amount of MNPs in the film. It was obvious that when increasing strength of the magnetic field, the in-plane m_r/m_s increased whereas the out-of-plane m_r/m_s decreased. This phenomenon was consistent with our observation for the cast films (**Figure 3b** and **3c**), suggesting that the electrodeposited MNP-chitosan film was more easily magnetized and directionally aligned in the film plane with increasing field. This also contributed to the increase of in-plane m_r when increasing the strength of the external magnetic field as shown in **Figure 4a**. In summary, adjusting the strength of the magnetic field during electrodeposition resulted in the tuning of magnetic properties of the electrodeposited MNP-chitosan films in both in-plane and out-of-plane directions.

(a)

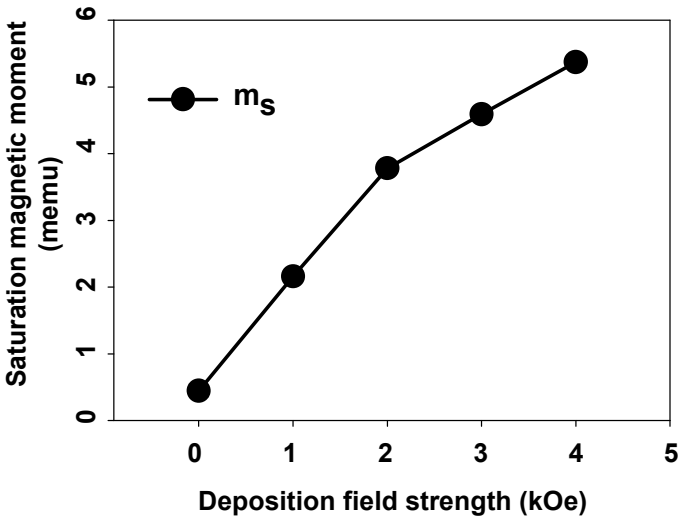
Saturation magnetic moment (memu)
0
1
2
3
4
5
6
m_S
0
1
2
3
4
5
Deposition field strength (kOe)

(b)

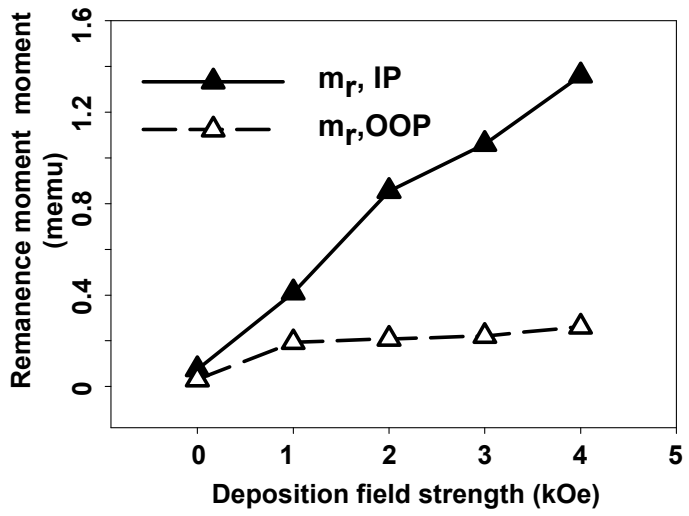
Remanence moment moment (memu)
0
0.4
0.8
1.2
1.6
m_r, IP
m_r,OOP
0
1
2
3
4
5
Deposition field strength (kOe)

(c)

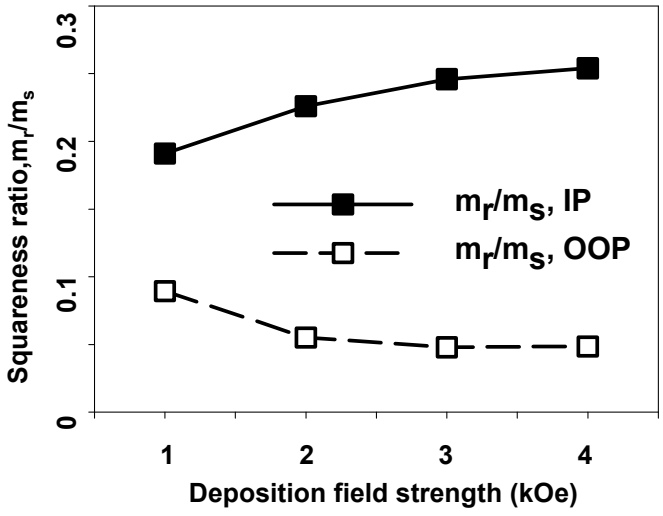
Squareness ratio,m_r/m_s
0
0.1
0.2
0.3
m_r/m_S, IP
m_r/m_S, OOP
1
2
3
4
Deposition field strength (kOe)

Figure 4. (a)Total saturation magnetic moment (m_s) of electrodeposited film as a function of the strength of applied magnetic field. (b) The remanence moment (m_r) of the electrodeposited film in the in-plane and out-of-plane direction as a function of the strength of external magnetic field. (c) The squareness ratio (m_r/m_s) of electrodeposition films as a function of the strength of external magnetic field. IP, in-plane; OOP, out-of-plane.

3.3.2.2 The effect of deposition time on magnetic properties of electrodeposited films

The unique feature of electrodeposition of chitosan lies in the fact that the electrodeposited films can be spatiotemporally controlled.[38] Here we examine the effect of deposition time[3, 17] on the magnetic properties of the MNP-chitosan films. The MNP-chitosan films were prepared by electrodepositing (3 A/m^2) MNP-chitosan solution (0.8 mg/ml) for 1 to 4 min in the presence of a magnetic field (1 kOe). **Figure 5a** and **b** show that the m_s, in-plane m_r and out-of-plane m_r of the MNP-chitosan film increase as a function of deposition time. Since the thickness of the electrodeposited chitosan film depends on the deposition time,[3, 9, 16] more MNPs could be incorporated into the chitosan film over time, resulting in the increased m_s and m_r in both in-plane and out-of-plane directions for the film. However, m_r/m_s remain nearly constant for varied deposition time (**Figure 5c**), possibly because this parameter mainly responded to the strength of magnetic field.

In summary, **Figure 3, 4** and **5** demonstrate that magnetic properties of the MNP-chitosan films can be tuned by adjusting the strength of magnetic field during film preparation processes.

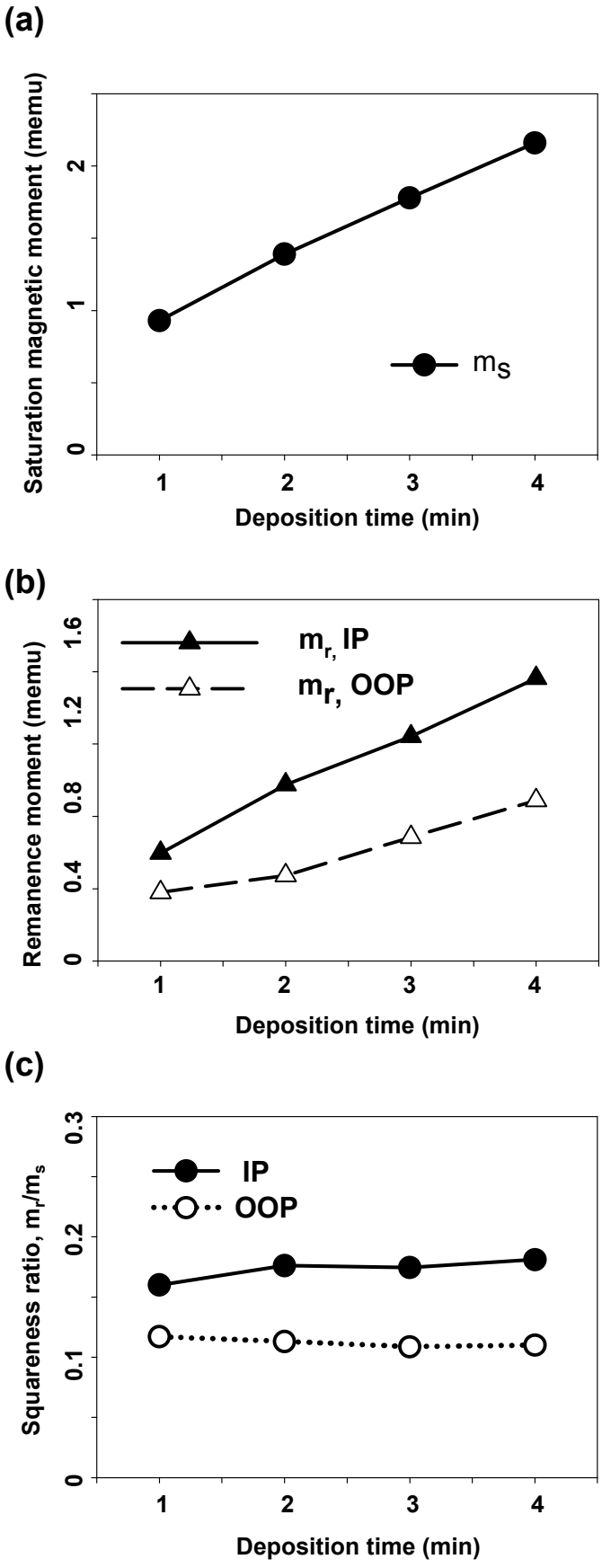
(a)
Saturation magnetic moment (memu)
0
1
2
m_S
1
2
3
4
Deposition time (min)
(b)
Remanence moment (memu)
0
0.4
0.8
1.2
1.6
$m_{r,}$ IP
$m_{r,}$ OOP
1
2
3
4
Deposition time (min)
(c)
Squareness ratio, m_r/m_s
0
0.1
0.2
0.3
IP
OOP
1
2
3
4
Deposition time (min)

Figure 5. The effects of deposition time on the (a) m_s, (b) m_r and (c) m_r/m_s of the MNP-chitosan films electrodeposited in the presence of a magnetic field of 1 kOe. IP, in-plane; OOP, out-of-plane.

3.4 Magnetic interactions between functionalized magnetic particles and MNP-chitosan films

The assembly/collection of biomaterial-conjugated magnetic microparticles (MMPs) by the magnetic aligned MNP-chitosan film was performed to demonstrate its reversible application.

3.4.1 Magnetic attractions between MMP-EGFP and casted MNP-chitosan film

We performed initial studies using casted films to demonstrate the magnetic attractions between MMPs and the MNP-chitosan films. Because the total magnetic moments (m_s and m_r) of the MNP-chitosan films are sensitive to the concentration of MNPs, the use of casted films precludes differences due to MNP concentration.

Firstly, carboxyl-functionalized MMPs were synthesized by a hydrothermal reaction of ferric ammonium citrate, hydrazine monohydrate and poly (acrylic acid).[39] The size, composition and magnetic properties of the MMPs can be found in **Figure S1b, d** and **e**, respectively. Secondly, EGFP was conjugated on MMPs through a carboxyl activating agent 1-ethyl-3-(3-dimethylaminopropyl) carbodiimide (EDC) (see **Experimental section 2.4**). Successful conjugation of EGFP to the MMPs is shown in **Figure S3**. Thirdly, three cast films were prepared by dropping 20 µl of corresponding solution onto a metal substrate. During the film formation, the MNP-chitosan film (casted using 2mg/mL MNP in chitosan suspension) with magnetic alignment was exposed to a magnetic field of 1 kOe, whereas the film without magnetic alignment was not exposed to an external magnetic field. A chitosan-only film was

also prepared. As shown in **Figure 6a**, the MMP-EGFP suspension (60 μl) was flowed on the magnetically aligned film, the non-aligned film, and the chitosan only film, respectively. After 30 sec of contact, the films were rinsed with deionized water for 3 times. The images of these films were taken in GFP filter using an Olympus MVX10 MacroView microscope equipped with an Olympus DP72 digital camera. Representative fluorescence microscopic images of these films after each treatment are shown in **Figure S4**. The fluorescent area of each film was analyzed by ImageJ software (rsb.info.nih.gov/ij) using the same color threshold.

Figure 6b shows that the total fluorescent area (i.e. working signal) of the magnetically aligned film was 4.2 times and 5.5 times higher than that of the chitosan film and non-aligned film, respectively. This is expected because MMP-EGFP was attracted by the magnetically aligned MNP-chitosan film but not the non-aligned or chitosan only film. We provide explanations as follows. First, the higher value of M_r of a magnetic film indicates that higher magnetic energy is stored in the film to attract the magnetic materials around it by magnetic force.[40] As discussed in **Section 3.3.1**, the MNP-chitosan film with magnetic alignment had a higher M_r than the one without magnetic alignment. Second, because the MNP-chitosan film without magnetic alignment was not exposed to a magnetic field during preparation, the MNPs in the film were not magnetized, so the magnetic fields generated by these particles were very weak and pointed in different directions. Therefore, although there is a M_r value for the non-aligned films but their attraction to the MMP were not higher than the chitosan only (nonmagnetic) film.

3.4.2 Magnetic removal of MMP-EGFP from the casted MNP-chitosan film

To release the MMP-EGFP from the MNP-chitosan films (**Figure 6a** right most), the three films, the magnetically aligned and non-aligned films and the chitosan-only film, were immersed in water. A neodymium magnet was placed at a distance of 5 mm from the film for 5 min. The films were taken out for fluorescent imaging using the same microscope as mentioned in **Section 3.4.1**. As shown in the right most set of columns in **Figure 6b**, after magnetic removal of EGFP-MMPs, the fluorescent signal of the magnetically aligned film was reduced to 11.7% that of its working signal, and was not significantly different from that of the chitosan only film. This provided further evidence that the binding of MMP-EGFP and the aligned film was mainly through magnetic attraction. It is worth noting that magnetic removal of MMPs from the MNP-chitosan film using an external magnet did not disturb the alignment or magnetic field of the film because: 1) the magnetic moment of the MNPs will return to the original direction (easy axis) once the external magnetic field is removed. As discussed in **Section 3.3.1**, the applied field did not exceed the critical value for irreversible rotation of magnetic moment; and 2) The structure of the chitosan film is stable once the film is deposited, which keeps the MNPs in place.[3] Microscopic images in **Figure S5** provided evidence that morphology of a randomly selected region in a magnetic aligned MNP-chitosan film remained unchanged before and after removal of MMPs.

In summary, **Figure 6** shows that MNP-chitosan film has the capability of magnetic collection and that the magnetic alignment is important for this feature.

3.4.3 Magnetic attraction and removal of MMP-EGFP from the electrodeposited MNP-chitosan film

Similar to the phenomenon observed for the cast films, the magnetic attraction and removal of MMP-EGFP can also be observed for electrodeposited films (**Figure 6c**). The aligned electrodeposited films showed significantly higher working fluorescent signals than those of chitosan only film and electrodeposited film without magnetic alignment, respectively. After taking away most MMP-EGFP by a strong external magnet, the fluorescent signal of aligned film was reduced to 8.6% of the working signal. The residual fluorescent signals might arise from non-specific protein adsorption to the film, as discussed in **Section 3.4.1**. Nonetheless, the magnetic attraction of MMP-EGFP to the aligned electrodeposited MNP-chitosan film and its magnetic removal process demonstrates the potential for multiple cycles of collection and release, a valuable feature of a device interface.

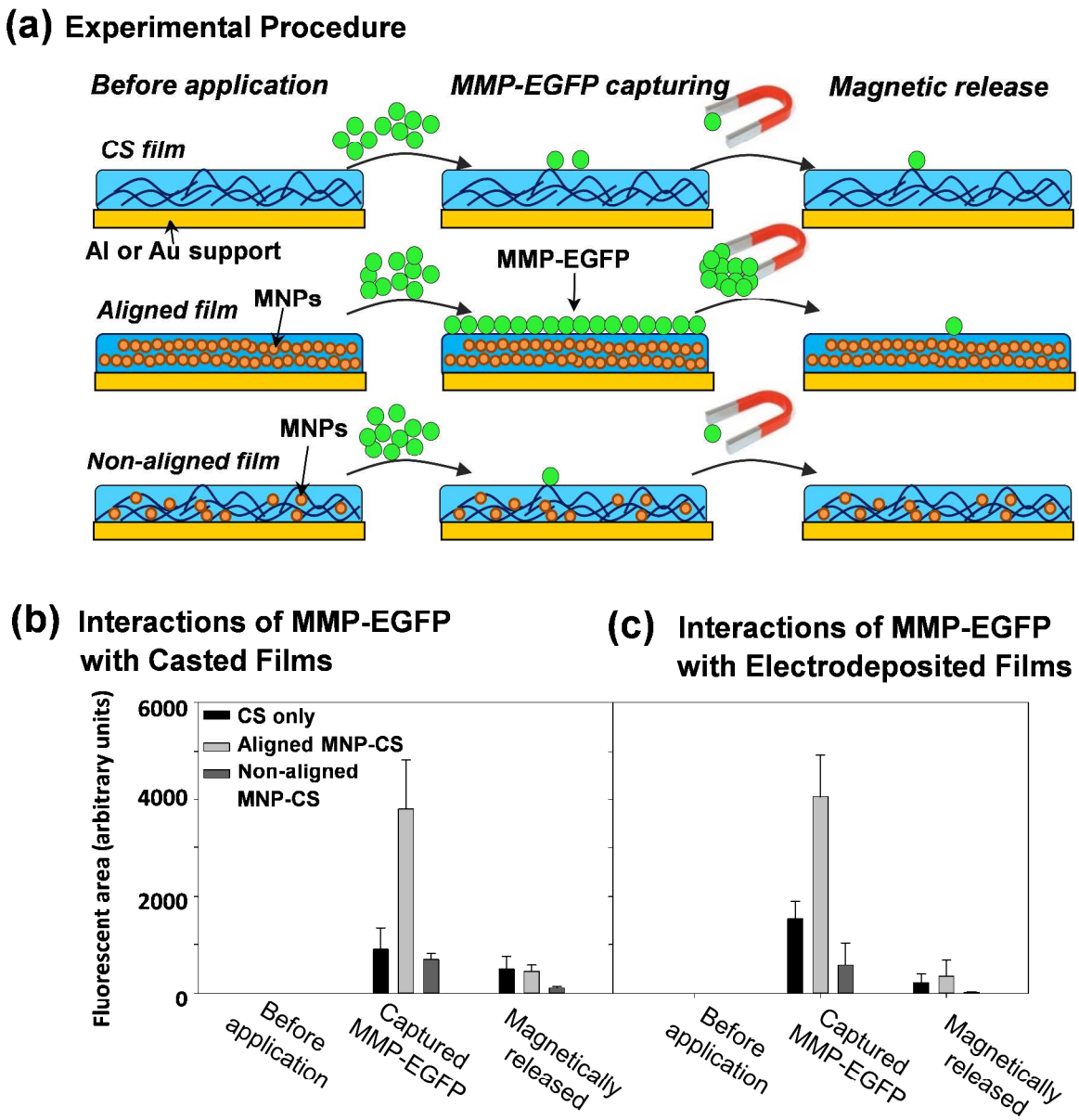

Figure 6 (a) Schematic illustration of experimental procedures for imaging magnetic interactions between EGFP-MMPs and the films. Both casted and electrodeposited films were tested following these procedures. (b) Interactions between MMP-EGFP and casted films. (c) Interactions between MMP-EGFP and electrodeposited films. The results were expressed as means ± standard deviation (n=3). Representative fluorescence microscopic images of (b) and (c) are shown in **Figure S4**. CS, chitosan.

3.5 Collection of bacteria by the aligned electrodeposited MNP-chitosan film

3.5.1 Cell capture using antibody-functionalized MMPs

E. coli cells were used to study the potential for bacterial capture using antibody-functionalized MMPs. A K-12 *E. coli* wildtype strain W3110 was used. **Figure 7a** demonstrates the coupling of MMPs to an anti-*E. coli* antibody using the EDC method (**Experimental section 2.4**). **Figure 7b** are the procedures for immunomagnetic separation of the cells. First, *E. coli* were inoculated in 10 mL of Luria Broth growth medium (Alfa Aesar) and grown at 37°C, under 250 rpm shaking until an OD_{600} of 1.0 was reached Then, the *E. coli* (20µl) were diluted in 5ml phosphate buffered saline (PBS, 0.1M, pH 7.0), and an MMP-antibody suspension (10 µl) was added. Two microliter of SYTO 9 green fluorescent nucleic acid stain (Life Technologies) was added to the mixtures to visualize the cells. Because of the selective binding of the antibody to the antigen cells, the MMP-antibody was able to specifically capture *E.coli* cells in the sample. After mixing for 15 min, the MMP-antibody and bound *E.coli* cells (MMP-*E. coli* complex) were attracted to the wall of the container by a magnet. The MMP-*E. coli* complexes were washed 3 times by repeated resuspension in 0.1M sterile PBS and magnetic collection. The washed MMP- *E. coli* complexes were suspended in 0.5 ml PBS and subjected to fluorescence microscopy. **Figure 7c** shows the co-localization of MMP-antibody and stained *E. coli* cells, indicating that the *E. coli* cells were captured by the MMP-antibody conjugates. In contrast, *E. coli* cells showed no attachment to the MMPs without antibody conjugation.

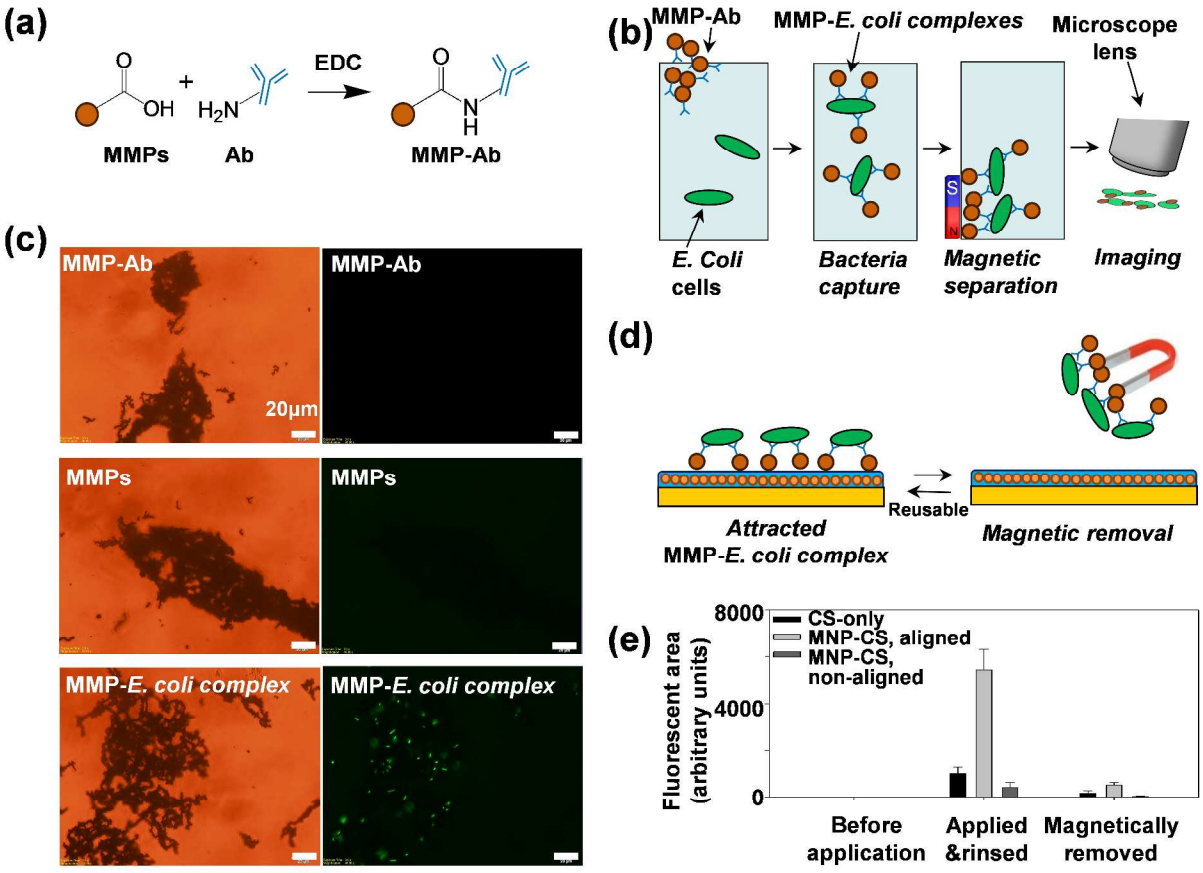

Figure 7. (a) Conjugation reaction of MMPs and antibody to form MMP-antibody conjugates using the EDC method. (b) Experimental procedures for immunomagnetic separation of *E.coli* by MMP-antibody. (c) *E. coli* cells (fluorescently stained) were captured by MMP-antibody conjugates but had little affinity to non-conjugated MMPs. The upper panel are the bright field and fluorescence microscopic images of MMP-antibody conjugates without adding *E.coli*. The middle and lower panels show the rinsed non-conjugated MMPs and MMP-antibody after adding *E.coli*, respectively. (d) Schematic illustration of collection and magnetic release of MMP-*E. coli* complexes on the aligned MNP-chitosan films. (e) Magnetic interactions of MMP-*E. coli* complexes with MNP-chitosan film with or without magnetic alignment and the chitosan

only film. The results were expressed as means ± standard deviation (n=3). CS, chitosan; Ab, antibody.

3.5.2 Collection of MMP-*E. coli* complexes using magnetically aligned MNP-chitosan film

In order to explore the feasibility of the MNP-chitosan film as a reversible biologically-based magnetic particle collector, the assembly and release of MMP-*E. coli* complex by the electrodeposited MNP-chitosan film is demonstrated. **Figure 7d** is the schematic illustration of collection and release of MMP-*E. coli* complexes by MNP-chitosan films. It depicts: 1) the magnetic attraction of MMP-*E. coli* complexes by the electrodeposited MNP-chitosan film with magnetic alignment, and 2) magnetic removal of MMP-*E. coli* complexes from the film by a stronger external magnet. Similar to the process of MMP-EGFP application, the MMP-*E.coli* complexes suspension was flowed on the surface of the films. After 30 sec, the films were rinsed with water 3 times and their fluorescent signals were examined. It can be seen in **Figure 7e** that a remarkably higher retention of MMP-*E.coli* complexes was observed on the magnetically aligned MNP-chitosan film than the controls (non-aligned film and chitosan only film).

To release the MMP-*E.coli* complexes from the magnetically aligned film, the film were placed in water and adjacent to a magnet (5mm away). All the films were subjected to microscopic imaging for fluorescent signals. In **Figure 7e** the fluorescent signals of MMP-*E.coli* complexes in the magnetically aligned film was greatly reduced. These results show the importance in the control of rapid collection and release of biological material in small localized environment (eg. microfluidic device interface).

4. CONCLUSIONS

Here we studied cathodic co-deposition from a suspension of chitosan and Fe_3O_4 nanoparticles and observed that the simultaneous imposition of a magnetic field during co-deposition can (i) organize structure, (ii) confer magnetic properties, and (iii) yield magnetic films that can perform reversible collection/assembly functions. As a proof of concept we demonstrate that the magnetic Fe_3O_4–chitosan films can reversibly collect/assemble magnetic particles that had been functionalized with proteins. We envision such magnetic films could have broad generic applications. For instance, magnetic chitosan films could provide a generic means to assemble enzyme-functionalized magnetic beads for biosensing applications. Alternatively, antibody-functionalized magnetic beads could be used to capture cells from a sample while magnetic collection could provide a means to separate and analyze these cells (e.g., for pathogen detection).

From the fabrication standpoint, this work demonstrates that top-down assembly methods using orthogonal cues (electrical and magnetic) can be coupled with bottom-up self-assembly to create soft matter with complex structure and properties. Importantly, fabrication of the magnetic Fe_3O_4–chitosan film is simple, rapid and reagentless.

ASSOCIATED CONTENT

Supporting Information.

The detailed synthesis procedures and characterization of the MNPs and MMPs, the procedures of conjugating enhanced green fluorescent protein (EGFP) to MMPs, the SEM images of MNPs and MMPs, magnetic hysteresis loops of MNPs and MMPs, X-ray diffraction pattern of the MNPs and MMPs, representative in-plane and out-of-plane hysteresis loops of casted and electrodeposited MNP-chitosan films with magnetic alignment, scheme of the

conjugation of MMPs and EGFP using carboxyl activating agent EDC, bright and EGFP filter images of MMPs with or without conjugation to EGFP, representative fluorescence microscopic images of interactions between MMP-EGFP and casted films and interactions between MMP-EGFP and electrodeposited films, bright field microscopic images of a randomly selected region in a magnetic aligned MNP-chitosan film before and after repeated magnetic removal of MMPs. These materials are available free of charge via the Internet at http://pubs.acs.org.

Funding Sources

The authors gratefully acknowledge financial support from the USDA-National Institute of Food Agriculture (No: 2014-67021-21585), National Science Foundation (CBET-1435957, CBET-1264509, CBET-1160005), and the Department of Defense, and Defense Threat Reduction Agency (HDTRA1-13-1-0037).

Notes

The authors declare no competing financial interest.

ACKNOWLEDGEMENTS

We acknowledge the support of the Maryland NanoCenter. Appreciation goes to Zi Teng, Juan Pablo Hurtado Padilla and Dr Wen-An Chiou for their professional assistance on SEM imaging. Appreciation also goes to Dr. Peter Zavalij for his kind interpretation on X-ray diffraction results.

ABBREVIATIONS

MNPs, magnetic nanoparticles; MMPs, magnetic microparticles; PDMS, polydimethylsiloxane; QCM, quartz crystal microbalance; SEM,; SEM-EDS, scanning electron microscopy with energy dispersive X-ray spectroscopy analysis; VSM, vibrating sample magnetometry; EGFP, enhanced green fluorescent protein; EDC, 1-ethyl-3-(3-dimethylaminopropyl) carbodiimide; MES, 2-(N-morpholino)-ethanesulfonic acid; Ab, antibody; M_r, remanent magnetization; M_s, saturation magnetization; H_c coercivity; m_s, the saturation magnetic moment; CS, chitosan; IP, in-plane; OOP, out-of-plane.

REFERENCES

1. Rybtchinski, B., Adaptive Supramolecular Nanomaterials Based on Strong Noncovalent Interactions. *ACS Nano* **2011,** *5* (9), 6791-6818.
2. Moore, J. S.; Kraft, M. L., Chemistry - Synchronized Self-assembly. *Science* **2008,** *320* (5876), 620-621.
3. Cheng, Y.; Gray, K. M.; David, L.; Royaud, I.; Payne, G. F.; Rubloff, G. W., Characterization of The Cathodic Electrodeposition of Semicrystalline Chitosan Hydrogel. *Mater. Lett.* **2012,** *87*, 97-100.
4. Ladet, S.; David, L.; Domard, A., Multi-membrane Hydrogels. *Nature* **2008,** *452* (7183), 76-9.
5. Xiong, Y.; Yan, K.; Bentley, W. E.; Deng, H.; Du, Y.; Payne, G. F.; Shi, X. W., Compartmentalized Multilayer Hydrogel Formation Using a Stimulus-Responsive Self-Assembling Polysaccharide. *ACS Appl Mater Interfaces* **2014,** *6* (4), 2948-57.
6. Dai, H. J.; Li, X. F.; Long, Y. H.; Wu, J. J.; Liang, S. M.; Zhang, X. L.; Zhao, N.; Xu, J., Multi-Membrane Hydrogel Fabricated by Facile Dynamic Self-Assembly. *Soft Matter* **2009,** *5* (10), 1987-1989.
7. Ladet, S. G.; Tahiri, K.; Montembault, A. S.; Domard, A. J.; Corvol, M. T. M., Multi-Membrane Chitosan Hydrogels as Chondrocytic Cell Bioreactors. *Biomaterials* **2011,** *32* (23), 5354-5364.
8. He, M.; Zhao, Y. T.; Duan, J. J.; Wang, Z. G.; Chen, Y.; Zhang, L. N., Fast Contact of Solid-Liquid Interface Created High Strength Multi-Layered Cellulose Hydrogels with Controllable Size. *ACS Appl. Mater. Interfaces* **2014,** *6* (3), 1872-1878.
9. Wu, L. Q.; Gadre, A. P.; Yi, H. M.; Kastantin, M. J.; Rubloff, G. W.; Bentley, W. E.; Payne, G. F.; Ghodssi, R., Voltage-Dependent Assembly of The Polysaccharide Chitosan onto an Electrode Surface. *Langmuir* **2002,** *18* (22), 8620-8625.

10. Redepenning, J.; Venkataraman, G.; Chen, J.; Stafford, N., Electrochemical Preparation of Chitosan/Hydroxyapatite Composite Coatings on Titanium Substrate. *J. Biomed. Mater. Res., Part A* **2003,** *66* (2), 411-6.
11. Luo, X. L.; Xu, J. J.; Du, Y.; Chen, H. Y., A Glucose Biosensor Based on Chitosan-Glucose Oxidase-Gold Nanoparticles Biocomposite Formed by One-Step Electrodeposition. *Anal. Biochem.* **2004,** *334* (2), 284-289.
12. Luo, X. L.; Xu, J. J.; Wang, J. L.; Chen, H. Y., Electrochemically Deposited Nanocomposite of Chitosan and Carbon Nanotubes for Biosensor Application. *Chem. Commun.* **2005,** (16), 2169-2171.
13. Pang, X.; Zhitomirsky, I., Electrodeposition of Composite Hydroxyapatite-Chitosan Films. *Mater Chem Phys* **2005,** *94* (2-3), 245-251.
14. Zangmeister, R. A.; Park, J. J.; Rubloff, G. W.; Tarlov, M. J., Electrochemical Study of Chitosan Films Deposited from Solution at Reducing Potentials. *Electrochim. Acta* **2006,** *51* (25), 5324-5333.
15. Fernandes, R.; Wu, L. Q.; Chen, T. H.; Yi, H. M.; Rubloff, G. W.; Ghodssi, R.; Bentley, W. E.; Payne, G. F., Electrochemically Induced Deposition of a Polysaccharide Hydrogel onto A Patterned Surface. *Langmuir* **2003,** *19* (10), 4058-4062.
16. Cheng, Y.; Luo, X. L.; Betz, J.; Buckhout-White, S.; Bekdash, O.; Payne, G. F.; Bentley, W. E.; Rubloff, G. W., In Situ Quantitative Visualization and Characterization of Chitosan Electrodeposition with Paired Sidewall Electrodes. *Soft Matter* **2010,** *6* (14), 3177-3183.
17. Liu, Y.; Zhang, B.; Gray, K. M.; Cheng, Y.; Kim, E.; Rubloff, G. W.; Bentley, W. E.; Wang, Q.; Payne, G. F., Electrodeposition of a Weak Polyelectrolyte Hydrogel: Remarkable Effects of Salt on Kinetics, Structure and Properties. *Soft Matter* **2013,** *9*, 2703-2710.
18. Zhang, Y. C.; Ji, C., Electro-Induced Covalent Cross-Linking of Chitosan and Formation of Chitosan Hydrogel Films: Its Application as an Enzyme Immobilization Matrix for Use in a Phenol Sensor. *Anal. Chem.* **2010,** *82* (12), 5275-5281.
19. Guo, M. Q.; Fang, H. D.; Wang, R.; Yang, Z. Q.; Xu, X. H., Electrodeposition of Chitosan-Glucose Oxidase Biocomposite onto Pt-Pb Nanoparticles Modified Stainless Steel Needle Electrode for Amperometric Glucose Biosensor. *J. Mater. Sci.-Mater. Med.* **2011,** *22* (8), 1985-1992.
20. Zhao, G.; Xu, J. J.; Chen, H. Y., Fabrication, Characterization of Fe3O4 Multilayer Film and Its Application in Promoting Direct Electron Transfer of Hemoglobin. *Electrochem. Commun.* **2006,** *8* (1), 148-154.
21. Bai, Y. H.; Du, Y.; Xu, J. J.; Chen, H. Y., Choline Biosensors Based on a Bi-Electrocatalytic Property of MnO2 Nanoparticles Modified Electrodes to H2O2. *Electrochem. Commun.* **2007,** *9* (10), 2611-2616.
22. Tangkuaram, T.; Ponchio, C.; Kangkasomboon, T.; Katikawong, P.; Veerasai, W., Design and Development of a Highly Stable Hydrogen Peroxide Biosensor on Screen Printed Carbon Electrode Based on Horseradish Peroxidase Bound with Gold Nanoparticles in The Matrix of Chitosan. *Biosens. Bioelectron.* **2007,** *22*, 2071-2078.
23. Wang, L.; Bao, J.; Wang, L.; Zhang, F.; Li, Y., One-Pot Synthesis and Bioapplication of Amine-Functionalized Magnetite Nanoparticles and Hollow Nanospheres. *Chem.-Eur. J.* **2006,** *12* (24), 6341-6347.
24. McRae, S. R.; Brown, C. L.; Bushell, G. R., Rapid Purification of EGFP, EYFP, and ECFP with High Yield and Purity. *Protein Expression Purif.* **2005,** *41* (1), 121-127.

25. Zhang, Y.; Sun, L.; Fu, Y.; Huang, Z. C.; Bai, X. J.; Zhai, Y.; Du, J.; Zhai, H. R., The Shape Anisotropy in the Magnetic Field-Assisted Self-Assembly Chain-like Structure of Magnetite. *J. Phys. Chem. C* **2009,** *113* (19), 8152-8157.
26. Kim, E.; Gordonov, T.; Bentley, W. E.; Payne, G. F., Amplified and in Situ Detection of Redox-Active Metabolite Using a Biobased Redox Capacitor. *Anal. Chem.* **2013,** *85* (4), 2102-2108.
27. Bertotti, G., *Hysteresis in Magnetism: For Physicists, Materials Scientists, and Engineers*. Academic Press: San Diego, California, USA, **1998**; p 3-6.
28. Liu, F.; Umlor, M. T.; Shen, L.; Weston, J.; Eads, W.; Barnard, J. A.; Mankey, G. J., The Growth of Nanoscale Structured Iron Films by Glancing Angle Deposition. *J. Appl. Phys.* **1999,** *85* (8), 5486-5488.
29. Kang, S.; Jia, Z.; Shi, S.; Nikles, D. E.; Harrell, J., Easy Axis Alignment of Chemically Partially Ordered Fept Nanoparticles. *Appl. Phys. Lett.* **2005,** *86* (6), 062503.
30. Fragouli, D.; Das, A.; Innocenti, C.; Guttikonda, Y.; Rahman, S.; Liu, L.; Caramia, V.; Megaridis, C. M.; Athanassiou, A., Polymeric Films with Electric and Magnetic Anisotropy Due to Magnetically Assembled Functional Nanofibers. *ACS Appl. Mater. Interfaces* **2014,** *6* (6), 4535-4541.
31. Suliţanu, N. D., Electrochemical Deposition of Novel Nanostructured Magnetic Thin Films for Advanced Applications. *Mater. Sci. Eng., B* **2002,** *95* (3), 230-235.
32. Ge, S.; Li, C.; Ma, X.; Li, W.; Xi, L.; Li, C. X., Approach to Fabricating Co Nanowire Arrays with Perpendicular Anisotropy: Application of a Magnetic Field During Deposition. *J. Appl. Phys.* **2001,** *90* (1), 509-511.
33. Chantrell, R.; Bradbury, A.; Popplewell, J.; Charles, S., Particle Cluster Configuration in Magnetic Fluid. *J. Phys. D: Appl. Phys.* **1980,** *13* (7), L119.
34. Skomski, R.; Hadjipanayis, G.; Sellmyer, D. J., Effective Demagnetizing Factors of Complicated Particle Mixtures. *IEEE Trans. Magn.* **2007,** *43* (6), 2956-2958.
35. Krycka, K. L.; Borchers, J. A.; Booth, R. A.; Ijiri, Y.; Hasz, K.; Rhyne, J. J.; Majetich, S. A., Origin of Surface Canting within Fe_3O_4 Nanoparticles. *Phys. Rev. Lett.* **2014,** *113* (14), 147203.
36. Bulte, D. P.; Langman, R. A., Origins of The Magnetomechanical Effect. *J. Magn. Magn. Mater.* **2002,** *251* (2), 229-243.
37. Cao, Q.; Han, X.; Li, L., Numerical Analysis of Magnetic Nanoparticle Transport in Microfluidic Systems under The Influence of Permanent Magnets. *J. Phys. D: Appl. Phys.* **2012,** *45* (46), 465001.
38. Wu, L.-Q.; Lee, K.; Wang, X.; English, D. S.; Losert, W.; Payne, G. F., Chitosan-Mediated and Spatially Selective Electrodeposition of Nanoscale Particles. *Langmuir* **2005,** *21* (8), 3641-3646.
39. Liu, X.; Hu, Q.; Fang, Z.; Wu, Q.; Xie, Q., Carboxyl Enriched Monodisperse Porous Fe_3O_4 Nanoparticles with Extraordinary Sustained-Release Property. *Langmuir* **2009,** *25* (13), 7244-7248.
40. Stefanita, C.-G., Magnetism: Basics and Applications. Springer: Burlington, MA, USA, p 21-24.

Table of Contents